



## Caffeic acid phenethyl ester (CAPE), an active component of propolis, inhibits *Helicobacter pylori* peptide deformylase activity

Kunqiang Cui<sup>a,1</sup>, Weiqiang Lu<sup>a,1</sup>, Lili Zhu<sup>a,1</sup>, Xu Shen<sup>a,b</sup>, Jin Huang<sup>a,\*</sup>

<sup>a</sup> Shanghai Key Laboratory of New Drug Design, Shanghai Key Laboratory of Chemical Biology, School of Pharmacy, East China University of Science and Technology, Shanghai 200237, PR China

<sup>b</sup> Shanghai Institute of Materia Medica, Chinese Academy of Sciences, Shanghai 201203, PR China

### ARTICLE INFO

#### Article history:

Received 1 April 2013

Available online 20 April 2013

#### Keywords:

*Helicobacter pylori*

Peptide deformylase

Propolis

Phenolic compounds

Caffeic acid phenethyl ester

### ABSTRACT

*Helicobacter pylori* (*H. pylori*) is a major causative factor for gastrointestinal illnesses, *H. pylori* peptide deformylase (HpPDF) catalyzes the removal of formyl group from the N-terminus of nascent polypeptide chains, which is essential for *H. pylori* survival and is considered as a promising drug target for anti-*H. pylori* therapy. Propolis, a natural antibiotic from honeybees, is reported to have an inhibitory effect on the growth of *H. pylori* in vitro. In addition, previous studies suggest that the main active constituents in the propolis are phenolic compounds. Therefore, we evaluated a collection of phenolic compounds derived from propolis for enzyme inhibition against HpPDF. Our study results show that Caffeic acid phenethyl ester (CAPE), one of the main medicinal components of propolis, is a competitive inhibitor against HpPDF, with an IC<sub>50</sub> value of 4.02 μM. Furthermore, absorption spectra and crystal structural characterization revealed that different from most well known PDF inhibitors, CAPE block the substrate entrance, preventing substrate from approaching the active site, but CAPE does not have chelate interaction with HpPDF and does not disrupt the metal-dependent catalysis. Our study provides valuable information for understanding the potential anti-*H. pylori* mechanism of propolis, and CAPE could be served as a lead compound for further anti-*H. pylori* drug discovery.

Crown Copyright © 2013 Published by Elsevier Inc. All rights reserved.

### 1. Introduction

*Helicobacter pylori* (*H. pylori*), is associated with numerous human diseases, such as mucosa-associated lymphoid tissue lymphoma, chronic gastritis, peptic ulcer, and gastric cancer [1–3]. Currently, more than half of human population worldwide is infecting with *H. pylori*, which has been recognized as one of the most prevalent human pathogens [4]. The primary factor interfering with the efficacy of current therapeutic regimens for *H. pylori* infection is the increasing prevalence of *H. pylori* antibiotic resistance [5]. Combination therapy, has been used as favorable treatment [6]. Nevertheless, the undesired adverse effects caused by this treatment are severe [7]. Therefore, developing novel

antibiotics that acting at new targets or via distinct modes is most likely to overcome the obstacle.

Peptide deformylase (PDF, EC 3.5.1.88), a member of a unique subclass of metalloenzymes, catalyzes the hydrolytic removal of the N-terminal formyl group from methionine residues following protein synthesis [8,9]. PDF is essential for bacterial growth but not required by eukaryotes, which imply an attractive target for developing new antibacterial agents [10,11], and a large amount of data indicate that PDF inhibitors (PDIs) act as broad-spectrum antibacterial agents [12–14]. To date, the majority of reported PDIs are pseudopeptide, including hydroxamic acids (e.g., actinonin, VRC-3375, VRC-4307), N-formyl hydroxylamine (e.g., LBM-415, BB-3497, BB-83698 and GSK1322322), and thiol peptides [15]. LBM-415, BB-83698 [15], and GSK1322322 [12] (Supplementary Material Fig. 1) have entered clinical trials, whereas most of pseudopeptidic compounds with low specificity for matrix metalloproteins and poor metabolic stability, that is putting forward an urgent need for the identification of novel and structurally diverse non-peptidic PDIs.

Natural products have been considered as crucial sources for lead compounds in discovering new drugs in the last few decades [16]. As a result of their structural diversity and uniqueness, natural products exhibit a broad range of biological activities. Propolis

**Abbreviations:** CAPE, caffeic acid phenethyl ester; PDF, peptide deformylase; HpPDF, *Helicobacter pylori* PDF; PDIs, peptide deformylase inhibitors; FDH, formate dehydrogenase; f-MAS, N-formyl-Met-Ala-Ser.

\* Corresponding author. Address: Shanghai Key Laboratory of New Drug Design, Shanghai Key Laboratory of Chemical Biology, School of Pharmacy, East China University of Science and Technology, 130 Mei Long Road, Shanghai 200237, PR China. Fax: +86 21 64253681.

E-mail address: [huangjin@ecust.edu.cn](mailto:huangjin@ecust.edu.cn) (J. Huang).

<sup>1</sup> These authors contributed equally to this work.

is a resinous material collected by bees from exudates and buds of the selected plants and mixed with wax and bee enzymes [17], and is widely used as antioxidant, anti-inflammatory, antibacterial, antiviral, anticancer and antifungal agent [18–23]. A number of researches have reported the anti-*H. pylori* activity of propolis [24,25]. Moreover, the antibacterial activity of propolis has been reported to be mainly correlated with phenolic compounds [26,27], which are structurally distinct from pseudopeptide.

On the basis of the above observations, it appears that phenolic compounds in propolis may be responsible for the anti-*H. pylori* activity of propolis. In this study, we evaluated 15 phenol-based compounds (Table 1, Fig. 1) derived from propolis, for their inhibitory activity against HpPDF. CAPE was identified as the most potent inhibitor among the 15 compounds. We then carried out inhibition mode analysis, absorption spectra and crystal structure characterization of HpPDF–CAPE complex. The results suggested that the binding mode of CAPE was different from most PDIs, with no chelation between the compound and the active site cobalt, which may lead to less adverse effects which caused by interactions with other metalloenzymes in human bodies. We believe that the inhibitory effect of CAPE against HpPDF may be one of the possible interpretations for propolis's inhibitory activity against *H. pylori* and it may be useful to develop and design a new class of PDIs.

## 2. Materials and methods

### 2.1. Materials

All the phenolic compounds for screening were obtained from Sigma–Aldrich or J&K. The purity of the compounds were  $\geq 95\%$ . NAD<sup>+</sup>, bovine serum albumin (BSA), and formate dehydrogenase (FDH) were obtained from Sigma; N-formyl-Met-Ala-Ser (f-MAS) was obtained from Invitrogen.

### 2.2. Protein expression and purification

Recombinant protein was overexpressed and purified as described previously [28]. The recombinant clone pET-22b-HpPDF was transformed into *E. coli* BL21(DE3). Transformed bacteria were grown overnight at 37 °C in LB media supplemented with 100 µg/ml ampicillin and diluted 1:50 (v/v) in fresh medium with the same antibiotic concentrations at 37 °C until OD<sub>600</sub> reached  $\sim 0.6$ . To prepare HpPDF enriched in a specific metal (Co, Ca, Mg, Ni, Zn), the culture was induced for an additional 6 h at 37 °C by the

addition of 0.5 mM IPTG and 0.1 mM of the desired metal (CoCl<sub>2</sub>, CaCl<sub>2</sub>, MgCl<sub>2</sub>, NiCl<sub>2</sub>, ZnCl<sub>2</sub>). The cells were harvested by centrifugation and suspended in buffer A (20 mM Tris–HCl, pH 8.0, 300 mM NaCl, and 10 mM imidazole). After sonication treatment on ice, the mixture was centrifuged to yield a clear supernatant, which was loaded onto a column with Ni-NTA resin (Novagen) pre-equilibrated in buffer A. The column was washed with buffer B (20 mM Tris–HCl, pH 8.0, 300 mM NaCl, and 20 mM imidazole) for several times and eluted with buffer C (20 mM Tris–HCl, pH 8.0, 300 mM NaCl, and 200 mM imidazole), then the soluble HpPDF fractions were pooled and dialyzed against buffer D (20 mM Tris–HCl, pH 8.0, 100 mM NaCl) to remove imidazole. The HpPDF was then concentrated using a 10 kDa centrifugal filter from Millipore. Protein concentration was determined by Bradford assay using bovine serum albumin (BSA) as a standard. All purification, dialysis, and concentration procedures were performed at 4 °C.

### 2.3. Inhibition screens

The enzymatic activity of HpPDF was evaluated using a FDH-coupled assay [29], in which the formate generated by PDF from its substrate N-formyl-Met-Ala-Ser (f-MAS) was oxidized by the enzyme FDH, reducing NAD<sup>+</sup> to NADH which causes specific absorption at 340 nm. All assays were conducted using a 96-well plate system and Synergy™ 4 Multi-Mode Microplate Reader (Bio-Tek). The assay buffer contained 50 mM HEPES, pH 7.5, 10 mM NaCl, 0.2 mg/ml BSA, 4 mM NAD<sup>+</sup>, 0.5 U/ml FDH and an appropriate concentration of HpPDF. The reaction was initiated by adding 2 mM f-MAS and absorbance at 340 nm was monitored for 5 min. 15 phenolic compounds were dissolved in DMSO at 50 mM as stock solutions. The enzyme was pre-incubated with 10 µM compounds for 10 min at room temperature and the activity was tested as described above. To determine the IC<sub>50</sub>s of the desired compounds, PDF activity was measured in the presence of increasing concentrations of the inhibitor. To investigate the inhibitor type, various concentrations of inhibitors were used, and the reaction was initiated by the addition of f-MAS (0.25–1.25 mM).

### 2.4. UV–vis absorption spectra

All absorption spectra were recorded on a Hitachi spectrophotometer (U-2910) at room temperature. PDF samples were prepared in buffer of 50 mM HEPES, pH 7.5, 10 mM NaCl. To gain insight into the mechanism of inhibition, spectra were recorded before and after the addition of inhibitor to the protein solution.

### 2.5. Protein crystallization and structure determination

Crystallization conditions for ligand-free PDF were screened by the hanging-drop method at 290 K using Hampton Research Crystal Screen, and Crystal Screen 2 (Hampton Research, Aliso Viejo, CA). A mixture of 1 µl protein solution and 1 µl reservoir solution was equilibrated against 500 µl reservoir solution. Well diffracting crystals were obtained in Crystal Screen 2 condition No. 35 (0.1 M HEPES pH 7.5, 70% v/v MPD). In order to obtain complex structures, soaking or co-crystallization study was undertaken. Both inhibitor stock solutions were prepared at 200 mM in 100% dimethyl sulfoxide.

X-ray diffraction data was collected at 100 K on beamline BL17U1 at Shanghai Synchrotron Radiation Facility (SSRF) and processed with HKL2000 [30]. Model building was performed in COOT [31] with the aid of the map sharpening utilities. The structure refinement was done using PHENIX [32] and Refmac 5 [33]. The figures were prepared using PyMOL [34]. Statistics for data processing and refinement are listed in Table 2. Hydrophobic interactions were analyzed using the LIGPLOT [35].

**Table 1**  
Inhibitions activity of phenolic compounds against HpPDF.

ID	Compounds	Inhibition (%) <sup>a</sup>	IC <sub>50</sub> (µM)
1	Caffeic acid	3.3	>100
2	Ferulic acid	8.0	>100
3	CAPE <sup>b</sup>	75	4.02
4	Chlorogenic acid	4.7	>100
5	Genistein	11.2	>100
6	Curcumin	0.1	>100
7	Naringenin	9.9	>100
8	Hesperitin	0.01	>100
9	Chrysin	1.8	>100
10	Apigenin	7.4	>100
11	Luteolin	5.9	>100
12	Kaempferol	0.2	>100
13	Myricetin	6.9	>100
14	Silibinin	4.9	>100
15	Rutin	0.02	>100
	Actinonin	95	0.17

<sup>a</sup> The inhibition rate was determined at the concentration of 10 µM.

<sup>b</sup> CAPE: caffeic acid phenethyl ester.

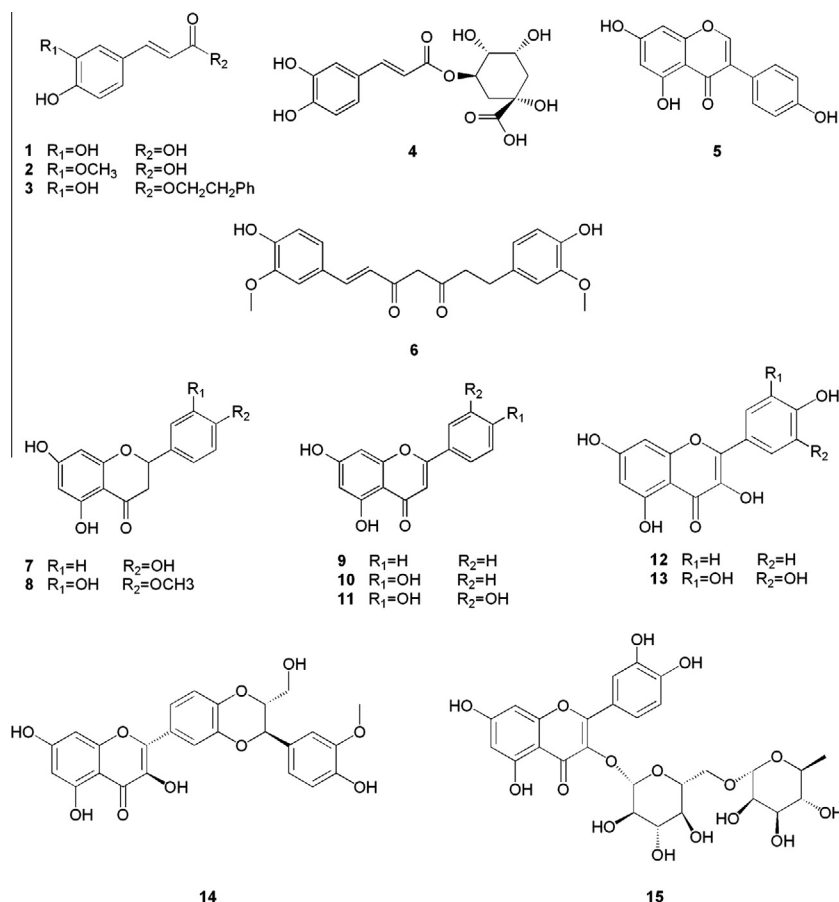


**Fig. 1.** Structures of phenolic compounds from propolis. The inhibitory activities against *HpPDF* of all the phenolic compounds were screened using a FDH-coupled assay.

### 3. Results and discussion

#### 3.1. Metal preference of *HpPDF*

The influence of the metal ions on the enzymatic activity of PDF from different species are diverse, e.g., *E. coli* PDF presents high activity with  $Fe^{2+}$  and  $Co^{2+}$  not  $Zn^{2+}$  [36], *B. cereus* PDF shows the same trend,  $Ni^{2+} > Co^{2+} > Zn^{2+}$  [37], *L. interrogans* PDF displays almost the opposite effect of  $Zn^{2+} > Fe^{2+} > Co^{2+} \sim Ni^{2+}$  [38]. To investigate metal dependence on *HpPDF* enzymatic activity,  $Zn^{2+}$ ,  $Co^{2+}$ ,  $Ca^{2+}$ ,  $Mg^{2+}$  and  $Ni^{2+}$  substituted enzymes were prepared by culturing *E. coli* cells in LB media supplemented with 100  $\mu M$   $ZnCl_2$ ,  $CoCl_2$ ,  $CaCl_2$ ,  $MgCl_2$ , and  $NiCl_2$ . The result shows the trend,  $Co^{2+} > -Ca^{2+} \sim Ni^{2+} > Zn^{2+} > Mg^{2+}$  (Supplementary Material Fig. 2), a similar trend as *E. coli* and *B. cereus*, the evolutionary diversity is expected to offer an explanation. Consequently, we prepared Co-*HpPDF* for studying *HpPDF* in this work.

#### 3.2. Inhibition screens

15 phenolic compounds from propolis were screened using the FDH-coupled assay to identify active compounds against *HpPDF* (Table 1). Actinonin, a naturally occurring PDI [39], presented a low  $IC_{50}$  value of 0.17  $\mu M$  (Fig. 2A). We used actinonin as a positive control to evaluate the inhibitors screening system. CAPE, one of the major components of propolis, was identified as a potential inhibitor of *HpPDF* with an  $IC_{50}$  value of 4.02  $\mu M$  (Fig. 2B). Kinetic analyses of active compounds against *HpPDF* were determined by the double-reciprocal (Lineweaver-Burk) plot, the lines intercepted on the  $1/v$  axis, indicating that both actinonin and CAPE are competitive inhibitors for the substrate f-MAS (Fig. 2C and D).

**Table 2**

Statistics of data collection and refinement.

	<i>HpPDF</i> -actinonin	<i>HpPDF</i> -CAPE
Data collection	–	–
Wavelength (Å)	0.98	0.98
Resolution (Å)	34.20–1.70	34.48–1.66
Space group	$P2_12_12_1$	$P2_12_12_1$
Cell dimensions	–	–
<i>a</i> , <i>b</i> , <i>c</i> (Å)	41.47, 51.97, 91.18	41.98, 52.24, 91.73
$\alpha$ , $\beta$ , $\gamma$ (°)	90, 90, 90	90, 90, 90
$R_{\text{sys}}$ or $R_{\text{merge}}$ (%)	0.080(0.080) <sup>a</sup>	0.082(0.082)
$I/\sigma(I)$	2.1	13.1
Completeness (%)	96.0	99.8
Redundancy	12.1	14.3
Refinement	–	–
Resolution (Å)	34.20–1.70	34.48–1.66
No. reflections	20249	22810
$R_{\text{work}}/R_{\text{free}}$	0.18/0.22	0.20/0.23
No. atoms	–	–
Protein	1309	1309
Cobalt ion	1	1
Inhibitor	21	27
Water	87	64
r.m.s.d. <sup>b</sup>	–	–
Bond lengths (Å)	0.009	0.011
Bond angles (°)	1.271	1.242
PDB code	4E9B	4E9A

<sup>a</sup> Values in parentheses are for highest-resolution shell.

<sup>b</sup> r.m.s.d., root mean square deviation.

#### 3.3. UV-vis absorption spectroscopy

Substitution of  $Co^{2+}$  for the native metal in a metalloenzyme provides a useful spectroscopic probe of the enzyme active-site

environment. This technique has previously been employed to successfully characterize numerous metalloenzymes [40–42]. To gain insight into the mechanism of inhibition, the *HpPDF*-inhibitor complexes were examined by UV–visible spectroscopy. As shown in Fig. 3 the electronic absorption spectrum of Co-*HpPDF* is similar to Co-*EcPDF* and Co-*BbPDF* [43,44]. It has an intense ligand-to-metal charge transfer band at  $\sim 330$  nm, indicating that the conserved cysteine in the EGCLS motif is ligated to the metal ion. In the visible region, PDF exhibits two d–d transition bands at 564 and 662 nm. Hydroxamic acid typically binds to the metal ion of metalloproteases as bidentate ligands, forming a penta-coordinate metal complex [37,45,46]. As presented in Fig. 3A, the addition of actinonin to PDF causes the decrease of magnitude at 564 nm, which is characteristic for the formation of a penta-coordinate complex, which has already been noticed in the case of Co-*EcPDF* in complex with actinonin [47]. The intensity of the absorbance at both 330 and 662 nm also decrease, we conclude that this is a strong evidence in favor of a charge transfer from the cobalt to the hydroxamate of actinonin [40]. The spectral characteristics of the CAPE-PDF complex (Fig. 3B) is very different from the actinonin-PDF complex, the intensity at 564 and 662 nm remained unaffected upon binding of CAPE, which indicates that the geometry of the metal does not change and environment of metal ion in the PDF has no significant change after the binding of CAPE. While the increase at 330 nm suggests that binding of CAPE enhances charge transfer from the Cys96 to cobalt. This observation suggests that the topology of the main chain backbone of *HpPDF* does not change, and the metal-dependent catalysis of PDF is also not be disrupted upon CAPE binding.

#### 3.4. Structural analysis of ligand–protein interactions

In order to gain the essential inhibition mechanism at the atomic level for actinonin and CAPE against *HpPDF*, we determined the

crystal structures of *HpPDF* in complex with actinonin and CAPE, respectively. In good agreement with their competitive inhibitory properties, both actinonin and CAPE locate near the active site and plug the substrate tunnel to prevent the substrate from accessing the catalytic site (Fig. 4A and B). Actinonin fits in the *HpPDF* active site in a linear conformation, of which both oxygen atoms of the hydroxamate moiety replacing the water molecule in the inhibitor free *HpPDF* structure, acts as a bidentate ligand. The spatial arrangement of the metal-coordinating residues does not change upon actinonin binding and in consequence  $\text{Co}^{2+}$  atom is penta-coordinated. The *n*-pentyl side chain of actinonin occupies the hydrophobic S1' pocket, which is formed by Gly44, Ile45, Tyr92, Leu131, Val134, and Ala135. In the S2' pocket that consist of Glu94 and Gly95, the isopropyl interacts with the carbons of Gly95 via Van der Waals interactions. The H-bond interaction residues for actinonin are Ile45, Gly46, Gln51, Lys93, Gly95, Leu97, and Glu139. Hydrophobic interactions are formed with Tyr103, Val134 and His138 (Fig. 4C and E). In the structure of *HpPDF*–CAPE complex, the head of CAPE (phenyl group) fits in the hydrophobic S1' pocket, and the tail expands to the pocket entrance. The carbonyl oxygen atom forms two hydrogen bonds to the hydrogen atoms of Ile45 and Gly46, respectively. Hydrogen bonds are also formed between the oxygen atom of 3-hydroxyl and the main-chain nitrogen atom of Gly101, Tyr103 and a water molecule. The two benzene rings make  $\pi$ – $\pi$  interactions with the side chain of Tyr103 and His138. CAPE also interacts with Glu94, Cys96, Leu97, Leu131, Ala135 and His138 through hydrophobic interactions (Fig. 4D and F). Actinonin represents the majority of known PDIs, which chelates the active site metal ion by hydroxamic or hydroxylamine part. However, there is no chelation between CAPE and the active site cobalt, which is different from most known PDIs. The main reason for the inhibition on *HpPDF* is CAPE block the substrate entrance, preventing substrate from approaching the active site.

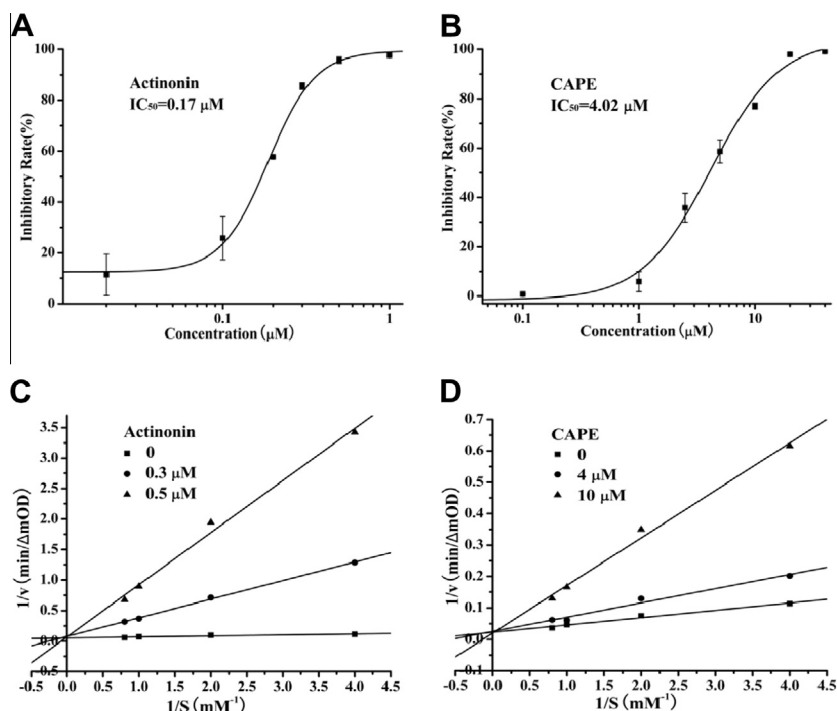


**Fig. 2.** Inhibitory properties of actinonin and CAPE. (A, B) Dose–response curves for enzyme inhibition by actinonin and CAPE, respectively. The  $\text{IC}_{50}$  value of inhibitor was estimated by fitting the inhibition data to the dose–response curve using a logistic derivative equation; (C, D) Lineweaver–Burk plots of *HpPDF* inhibited by actinonin and CAPE, respectively. The panel shows the representative double reciprocal plots of  $1/v$  vs  $1/S$  at different inhibitor concentrations. (C: ■, absence of inhibitor; ●, 0.3  $\mu\text{M}$  actinonin; ▲, 0.5  $\mu\text{M}$  actinonin. D: ■, absence of inhibitor; ●, 4  $\mu\text{M}$  CAPE; ▲, 10  $\mu\text{M}$  CAPE.)



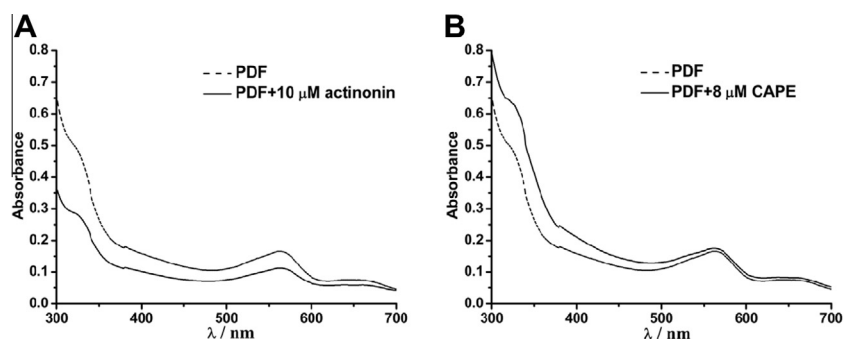


**Fig. 3.** Electronic absorption spectra of PDF-inhibitor complexes. (A, B) Binding of 10  $\mu$ M actinonin and 8  $\mu$ M CAPE to *Hp*PDF, respectively. The inhibitors themselves did not show spectral bands in the 300–700 nm range but CAPE give strong absorbance bands below 300 nm (spectrum not shown).

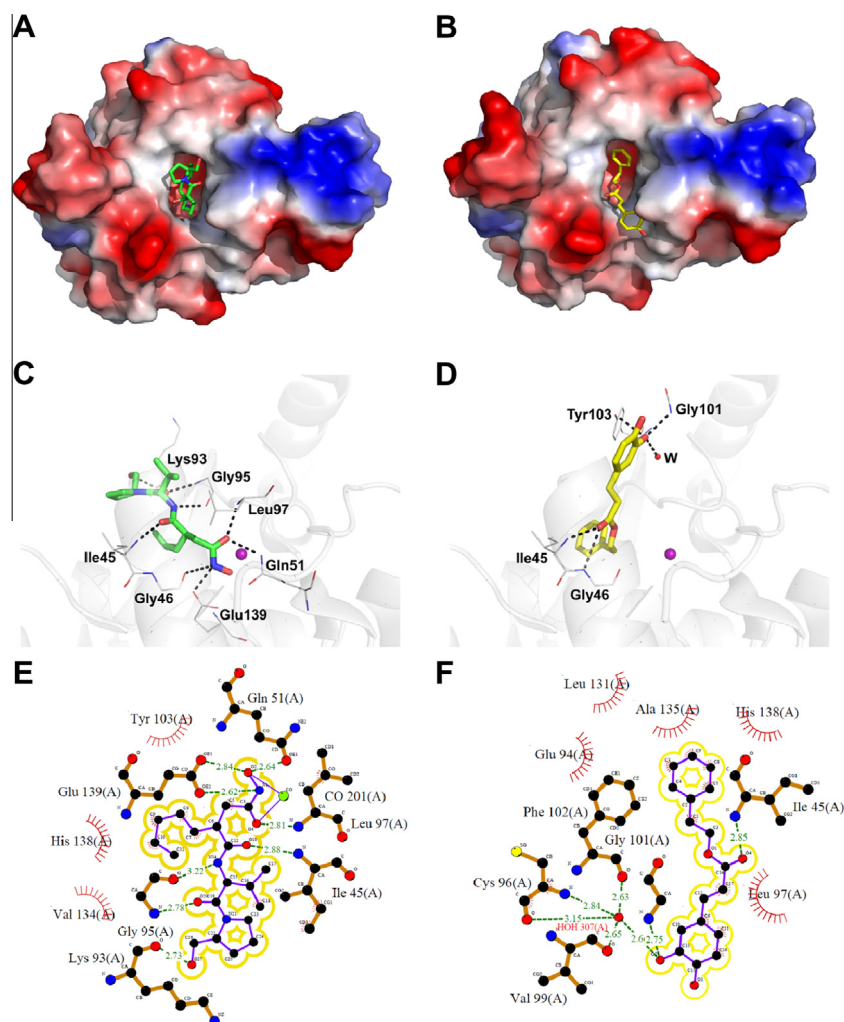


**Fig. 4.** Ribbon and stick 2D diagram of interaction between *Hp*PDF and inhibitors. (A, B) Binding positions of actinonin and CAPE around the substrate tunnel; (C, D) The nitrogen, oxygen, and sulfur atoms are colored blue, red, and yellow, respectively. The  $\text{Co}^{2+}$  ion in active site is represented by the pink sphere. The interactions between inhibitors and residues nearby, as well as some water molecules, are indicated. The bound water molecule is shown as red spheres. Black dotted lines represent the key hydrogen bonds involved in inhibitors binding. The carbons of protein and inhibitors are colored gray (PDF), green (actinonin) and yellow (CAPE), respectively; (E, F) The interactions were plotted with the computer program LIGPLOT. (For interpretation of the references to color in this figure legend, the reader is referred to the web version of this article.)

#### 4. Conclusion

The precise mechanism of propolis's pharmacological property responsible for anti-*H. pylori* effect is yet unclear. Dermot Kelleher's group demonstrated that CAPE had anti-inflammatory effects on *H. pylori*-infected gastric epithelial cells [48]. In this study, we

demonstrate that CAPE shows strong inhibitory activity against *Hp*PDF, which may account for the anti-*H. pylori* activity of propolis. Moreover, the structure of CAPE is different from the majority of known PDF inhibitors, which are mainly pseudopeptides. CAPE binds in the active site region without interaction with the catalytic  $\text{Co}^{2+}$ , which may decrease the interaction between CAPE and

other metalloproteins in human body and hence reduce the possible adverse effect. The study that we present here provides new structural information on inhibitor-*Hp*PDF complex, which will assist in designing new potential anti-*H. pylori* inhibitors and improving rational drug design.

## Acknowledgments

This work was supported by the National Natural Science Foundation of China (Grant 81102420), the Innovation Program of Shanghai Municipal Education Commission (Grant 10ZZ41), the Specialized Research Fund for the Doctoral Program of Higher Education of China (Grant 20090074120012), the Shanghai Committee of Science and Technology (Grant 11DZ2260600), and the Fundamental Research Funds for the Central Universities.

## Appendix A. Supplementary data

Supplementary data associated with this article can be found, in the online version, at <http://dx.doi.org/10.1016/j.bbrc.2013.04.026>.

## References

- [1] M. Kato, M. Asaka, *Jpn. J. Clin. Oncol.* 40 (2010) 828–837.
- [2] C.R.A. Motta, M.P.S.S. Cunha, D.M.M. Queiroz, F.W.S. Cruz, E.J.C. Guerra, R.M.S. Mota, L.L.B.C. Braga, *Digestion* 78 (2008) 3–8.
- [3] M. Plummer, L.J. Van Doorn, S. Franceschi, B. Kleter, F. Canzian, J. Vivas, G. Lopez, D. Colin, N. Muñoz, I. Kato, *J. Natl. Cancer I.* 99 (2007) 1328–1334.
- [4] J.C. Atherton, *Annu. Rev. Pathol. Mech. Dis.* 1 (2006) 63–96.
- [5] V. De Francesco, F. Giorgio, C. Hassan, G. Manes, L. Vannella, C. Panella, E. Ierardi, A. Zullo, *J. Gastrointest Liver Dis.* 19 (2010) 409–414.
- [6] S.A. Mirbagheri, M. Hasibi, M. Abouzari, A. Rashidi, *World J. Gastroentero.* 12 (2006) 4888–4891.
- [7] D. Carcanague, Y.K. Shue, M.A. Wuonola, M. Uria-Nickelsen, C. Joubran, J.K. Abedi, J. Jones, T.C. Kähler, *J. Med. Chem.* 45 (2002) 4300–4309.
- [8] J.A. Leeds, C.R. Dean, *Curr. Opin. Pharmacol.* 6 (2006) 445–452.
- [9] J.M. Adams, M.R. Capecchi, *Proc. Natl. Acad. Sci. USA* 55 (1966) 147–155.
- [10] K.T. Nguyen, X.B. Hu, C. Colton, R. Chakrabarti, M.X. Zhu, D.H. Pei, *Biochemistry-Moscow+* 42 (2003) 9952–9958.
- [11] Z.Y. Yuan, J. Trias, R.J. White, *Drug Discov. Today* 6 (2001) 954–961.
- [12] D.M. Livermore, M. Blaser, O. Carrs, G. Cassell, N. Fishman, R. Guidos, S. Levy, J. Powers, R. Norrby, G. Tillotson, *J. Antimicrob. Chemoth.* 66 (2011) 1941–1944.
- [13] R. Jain, D. Chen, R.J. White, D.V. Patel, Z. Yuan, *Curr. Med. Chem.* 12 (2005) 1607–1621.
- [14] S. Ramanathan-Girish, J. McColm, J.M. Clements, P. Taupin, S. Barrowcliffe, J. Hevizi, S. Safrin, C. Moore, G. Patou, H. Moser, A. Gadd, U. Hoch, V. Jiang, D. Lofland, K.W. Johnson, *Antimicrob. Agents Ch.* 48 (2004) 4835–4842.
- [15] D.R. Guay, *Ther. Clin. Risk Manag.* 3 (2007) 513–525.
- [16] A.L. Harvey, *Drug Discov. Today* 13 (2008) 894–901.
- [17] R.M. Darwish, R.J. Abu Fares, M.H. Abu Zarga, I.K. Nazer, *Afr. J. Biotechnol.* 9 (2010) 5966–5974.
- [18] C. Scully, *Br. Dent. J.* 200 (2006) 359–360.
- [19] M.A.E. Watanabe, M.K. Amarante, B.J. Conti, J.M. Sforcin, *J. Pharm. Pharmacol.* 63 (2011) 1378–1386.
- [20] N. Paulino, S.R.L. Abreu, Y. Uto, D. Koyama, H. Nagasawa, H. Hori, V.M. Dirsch, A.M. Vollmar, A. Scremin, W.A. Bretz, *Eur. J. Pharmacol.* 587 (2008) 296–301.
- [21] E.M.A.F. Bastos, M. Simone, D.M. Jorge, A.E.E. Soares, M. Spivak, *J. Invertebr. Pathol.* 97 (2008) 273–281.
- [22] W.M. Wu, L. Lu, Y. Long, T. Wang, L. Liu, Q. Chen, R. Wang, *Food Chem.* 105 (2007) 107–115.
- [23] S. Silici, N.A. Koç, D. Ayangil, S. Çankaya, *J. Pharmacol. Sci.* 99 (2005) 39–44.
- [24] M. Skiba, E. Szliszka, M. Kunicka, W. Krol, *Cent. Eur. J. Immunol.* 36 (2011) 65–69.
- [25] M. Biagi, E. Miraldi, N. Figura, A.R. Magnano, G. Ierardi, D. Manca, M. Corsini, B. Barlozzini, C. Mannari, C. Stiazzini, S. Sodano, D. Giachetti, *Planta Med.* 77 (2011). 1418–1418.
- [26] N. Kalogeropoulos, S.J. Konteles, E. Troullidou, I. Mourtzinis, V.T. Karathanos, *Food Chem.* 116 (2009) 452–461.
- [27] K.W. Jeong, J.Y. Lee, D.I. Kang, J.U. Lee, S.Y. Shin, Y. Kim, *J. Nat. Prod.* 72 (2009) 719–724.
- [28] C. Han, Q. Wang, L. Dong, H.F. Sun, S.Y. Peng, J. Chen, Y.M. Yang, J.M. Yue, X. Shen, H.L. Jiang, *Biochem. Biophys. Res. Commun.* 319 (2004) 1292–1298.
- [29] C. Lazennec, T. Meinnel, *Anal. Biochem.* 244 (1997) 180–182.
- [30] Z. Otwinowski, W. Minor, *Method Enzymol.* 276 (1997) 307–326.
- [31] P. Emsley, K. Cowtan, *Acta Crystallogr. D* 60 (2004) 2126–2132.
- [32] P.D. Adams, P.V. Afonine, G. Bunkoczi, V.B. Chen, I.W. Davis, N. Echols, J.J. Headd, L.W. Hung, G.J. Kapral, R.W. Grosse-Kunstleve, *Acta Crystallogr. D* 66 (2010) 213–221.
- [33] G.N. Murshudov, P. Skubák, A.A. Lebedev, N.S. Pannu, R.A. Steiner, R.A. Nicholls, M.D. Winn, F. Long, A.A. Vagin, *Acta Crystallogr. D* 67 (2011) 355–367.
- [34] W.L. DeLano, *Scientific*, San Carlos, CA, USA, (2002).
- [35] A.C. Wallace, R.A. Laskowski, J.M. Thornton, *Protein Eng.* 8 (1995) 127–134.
- [36] P.T.R. Rajagopalan, X.C. Yu, D. Pei, *J. Am. Chem. Soc.* 119 (1997) 12418–12419.
- [37] J.K. Park, K.H. Kim, A.H. Moon, E.E. Kim, *J. Biochem. and Mol. Biol.* 40 (2007) 1050–1057.
- [38] Y.K. Li, S.X. Ren, W.M. Gong, *Acta Crystallogr. D* 58 (2002) 846–848.
- [39] D.Z. Chen, D.V. Patel, C.J. Hackbarth, W. Wang, G. Dreyer, D.C. Young, P.S. Margolis, C. Wu, Z.J. Ni, J. Trias, *Biochemistry-Moscow+* 39 (2000) 1256–1262.
- [40] T. Meinnel, L. Patiny, S. Ragusa, S. Blanquet, *Biochemistry-Moscow+* 38 (1999) 4287–4295.
- [41] R.M. Breece, A. Costello, B. Bennett, T.K. Sigdel, M.L. Matthews, D.L. Tierney, M.W. Crowder, *J. Biol. Chem.* 280 (2005) 11074–11081.
- [42] C.E. Sabel, J.L. Shepherd, S. Siemann, *Anal. Biochem.* 391 (2009) 74–76.
- [43] P.T.R. Rajagopalan, S. Grimme, D.H. Pei, *Biochemistry-Moscow+* 39 (2000) 779–790.
- [44] K.T. Nguyen, J.C. Wu, J.A. Boylan, F.C. Gherardini, D. Pei, *Arch. Biochem. Biophys.* 468 (2007) 217–225.
- [45] H.J. Yoon, H.L. Kim, S.K. Lee, H.W. Kim, J.Y. Lee, B. Mikami, S.W. Suh, *Proteins* 57 (2004) 639–642.
- [46] S. Escobar-Alvarez, Y. Goldgur, G. Yang, O. Ouerfelli, Y.M. Li, D.A. Scheinberg, *J. Mol. Biol.* 387 (2009) 1211–1228.
- [47] S.K. Grant, B.G. Green, J.W. Kozarich, *Bioorg. Chem.* 29 (2001) 211–222.
- [48] M.M.M. Abdel-Latif, H.J. Windle, B.S.E. Homasany, K. Sabra, D. Kelleher, *Brit. J. Pharmacol.* 146 (2005) 1139–1147.